

INTERNATIONAL SOCIETY FOR SOIL MECHANICS AND GEOTECHNICAL ENGINEERING



This paper was downloaded from the Online Library of the International Society for Soil Mechanics and Geotechnical Engineering (ISSMGE). The library is available here:

<https://www.issmge.org/publications/online-library>

This is an open-access database that archives thousands of papers published under the Auspices of the ISSMGE and maintained by the Innovation and Development Committee of ISSMGE.

SECTION V

EARTH PRESSURE; STABILITY AND DISPLACEMENTS OF RETAINING CONSTRUCTIONS

SUB-SECTION V a

EARTH PRESSURE AGAINST RIGID VERTICAL WALLS

V a 6

EXPERIMENTAL STUDY OF THE PRESSURE EXERTED BY A PULVERULENT MASS AGAINST A RETENTION WALL

(Scale Model Tests)

J. GRADOR

SYNOPSIS OF THE FRENCH REPORT

The Paper is a report of a series of re-search experiments on soil pressure against a retention wall.

The tests were made on a very small scale model:

The height and width of the wall were respectively 50 and 80 cm. (19 1/2 and 31 inches).

The object of our research was to measure the distribution of the fill pressure against

the whole height of the retention wall.

The paper describes in detail the test devices which made these pressure measurements possible; they are an application of Mr. Coyne's general method for acoustic measurement of deformations. As for the test results, they confirm and clarify the non hydraulic nature of the active pressure of soils which has already been brought out by other experimental methods.

-o-o-o-o-o-o-

SUB-SECTION V b

EARTH PRESSURE AGAINST FLEXIBLE VERTICAL WALLS

V b 8 A REPORT OF FIELD AND LABORATORY TESTS ON THE STABILITY OF POSTS AGAINST LATERAL LOADS

WALTER L. SHILTS

LEROY D. GRAVES

GEORGE G. DRISCOLL

University of Notre Dame

SUMMARY

This report describes full scale field tests conducted for the Outdoor Advertising Association of America on the stability against lateral loads of the posts of their cantilever type advertising structures. In addition, it describes small scale laboratory tests conducted by the authors to check and complement the field tests. Field posts were tested in a granular soil and a silt-clay. Laboratory posts were tested in a clean fine sand. Field loads were applied to individual posts in increments to as much as 3000 pounds by use of a chain hoist and a dynamometer. Laboratory loads were applied by a cable, pulley, and weights. Deflections were measured with dial gauges and scales. The results are presented as plotted curves of the post deflection under load. Discussion of the results leads to the following conclusions:

1) The relation between the "average soil pressure" caused by a lateral load and the resulting post movement in a granular soil at the ground level is described by the equation:

$$\frac{Q_1}{A_1} = p_p \log (1 + 2 \Delta \tan \phi)$$

$\frac{Q_1}{A_1}$ is the "average soil pressure"

p_p is Rankine's passive pressure

Δ is the post movement

ϕ is the angle of interval friction of the soil

- 2) For an undisturbed cohesive soil, ϕ must be changed to a ϕ' which gives a passive pressure value at the bottom of the post equal to that using ϕ and the cohesion.
- 3) For remolded cohesive soil, both the coefficient and exponent of Δ must be made equal to one.
- 4) The point of rotation, for normal post depths, is at that depth below which there is 0.324 of the total vertical cross-sectional area of the embedded portion of the post.
- 5) The data presented in this report offers a rational method of designing posts and anchorages against relatively small movements under lateral loads.

INTRODUCTION

In the spring of 1947, the writers were asked by the Outdoor Advertising Association of America to conduct some full scale field tests of the stability of its cantilever type signboards under wind loads. Usually, each signboard consists of three posts, embedded in the soil, supporting a vertical poster face twelve feet high by twenty five feet long with the centre of the poster face being ten feet above ground. In the conference with the Association, it was decided that the most feasible plan of attack was to assume that wind loads were distributed equally to each post and that these equal loads could be replaced by a concentrated static load applied at the height of the centre of the poster face. These assumptions allowed each signboard to be represented by a single post in the field tests and each wind load to be applied at a height above ground of ten feet except for posts representing extra high signboards. As suggested by the Association, eight different posts were tested in a granular soil. The results of these tests showed the necessity for tests in another soil and five different posts were tested in a silt-clay soil. A report of the field tests was made to the Association in August, 1947. The analysis of the data in this report indicated some points about post stability that needed further investigation and the writers began a series of small scale laboratory tests using posts one fourth the field size embedded in a clean fine sand. The laboratory tests were designed to check the analysis of the field test results as to the location of the point of rotation and the effect of post shape on resistance to load. Both laboratory and field tests measured post stability at relatively small deflections rather than complete overturning. For a discussion of stability against complete overturning, the reader is referred to an article by J.F. Seiler entitled, "Effect of Depth of Embedment on Pole Stability" published in "Wood Preserving News" for November, 1932.

EMBEDMENT SOILS

Site Number 1: A soil profile of field site number one would show a thin sandy topsoil underlain by a sand which accumulates gravel and binder soil as the depth increases to form a "hardpan" layer at a depth of about four feet. Below this "hardpan" layer is a deep layer of fine, poorly graded gravel of low density. Pedologically, the soil would be classified as similar to the "Door" soils of the Wisconsin Drift Area. Details of gradation, density, and soil profile of this site are given in Figures 19 and 20.

Site Number 2: A soil profile of field test site number two would show a thin layer of topsoil underlain by about four feet of mottled gray-brown silt-clay soil. At a depth of about five feet a three inch layer of sand occurs and immediately under this is the parent layer of clay, silt, sand, and gravel in a hard, dense condition. Pedologically, the soil would be similar to the "Brookston" soils of the Wisconsin Drift Area. Details of gradation, plastic-

ity, density, strength, and soil profile of this site are given in Figures 21, 22, and 23 and in Table 4.

Laboratory: The fine sand used in the laboratory tests had an effective grain size of 0.18 mm and a uniformity coefficient of 1.63. The gradation was as follows:

Sieve Size	Per Cent Passing
4	100
8	99.4
16	99.2
30	98.4
50	72.1
80	9.4
100	5.1
200	0.4

It was used in an air dry condition and compacted to a density of approximately 107 pounds per cubic feet.

FIELD TESTING

Loading Equipment: The load was applied with a standard two-ton chain hoist fastened to a snub post by a long chain. The load was measured by a "Dillon Dynamometer" of 10,000 pound capacity in a specially built frame with eyebolts in opposing ends to allow the travel chain of the hoist to be hooked in one eyebolt and the other eyebolt to be fastened to an eyebolt protruding from a clamp on the test post. The clamp for the test post employed steel rods to hold two short pieces of 3 inch steel I-Beam on opposing sides of the post. Plate 1 shows a photograph of this equipment in use.

Deflection Measuring Equipment: Movement of the post and/or anchorage was measured at the top by means of a scale (1/8 inch graduations) clamped to the post and at points 2, 23, and 44 inches above ground by means of standard dial gauges of one inch travel and .001 inch graduations. The line of sight of a transit was used as the reference for measuring movement with the scale. The support and reference for the dial gauges consisted of two 2" x 4" wood stakes driven firmly in the ground to which was fastened a framework of light metal I-Beam and steel strap. A photograph of this equipment is shown in Plate 2.

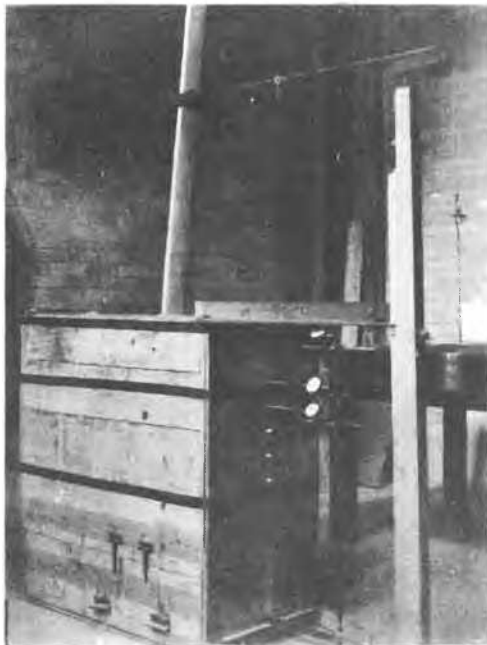
Procedure

Installation: Test posts were installed in a straight line 15 feet apart with the hole digging and backfilling being done in the normal manner employed in advertising structure erection. On opposing sides of the test posts, snub posts were installed on a line perpendicular to the test post line and 20 feet distant therefrom. These snub posts were anchored against the pull by 6 inch diameter screw anchors and cables. Details of the depth of embedment and size and shape of anchorage for each test post are given with the test results for that post.

Testing: When the post were ready to test, load was applied at a height equal to that of the centre of the poster face of the structure and in increments of 300 pounds up to a total of



Loading equipment on post 3
Plate 1



Laboratory testing equipment
Plate 3



Dial gauges and supports Post 12
Plate 2

1800 pounds and then 200 pounds up to 2,000 pounds after which the load was released. Deflections were read when the rate of deflection at the ground surface was .001 inch per minute or less for posts 1, 2, 3, and 5 and .002 inch per minute or less for all other posts. If the deflection at the ground surface was one-half inch or less at 2,000 pounds load or if other reasons made it expedient, the process of pulling by increments was repeated in the opposite direction. Then, if the deflection at the ground surface did not reach one-half inch, a load of 2,000 pounds was applied alternately in each direction for several cycles. At the end of the repetition cycles, the load was carried up to 2700 pounds and to 3000 pounds in some instances. If the deflection under the first loading by increments was greater than one-half inch at 2000 pounds, the load was increased to 2700 and sometimes to 3000 pounds. Post 5 was loaded in 200 pound increments.

Auxiliary Testing: Immediately after the test-

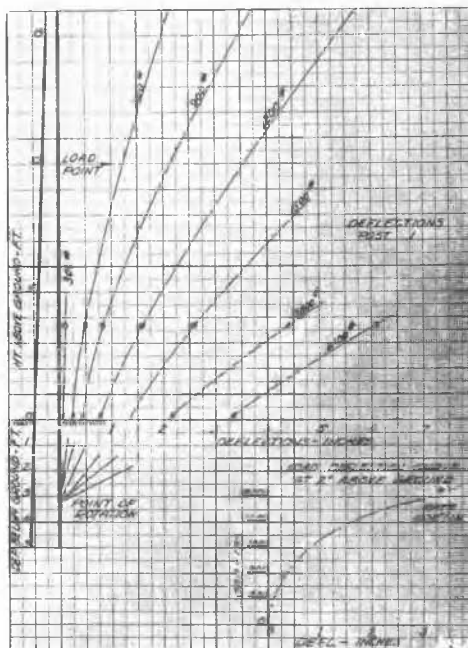


FIG. 1

ing of each post, a boring was made with a 4 inch soil auger in the soil adjacent to the post hole and moisture content samples were obtained for each foot of embedment of the post. After all posts were tested at each site, a test pit was dug and samples of each soil layer were obtained for analysis in the laboratory. Also after all posts were tested at each site, several "pilot auger" tests were made to tie the soil classification to that set up by Dr. P.C. Rutledge in a previous report to the Association on the pull-out resistance of soil anchors. These tests were made by turning a standard 1 1/2 inch soil auger into

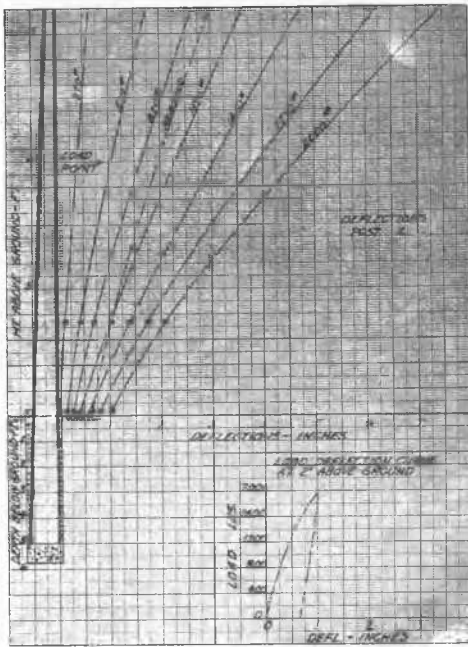


FIG. 2

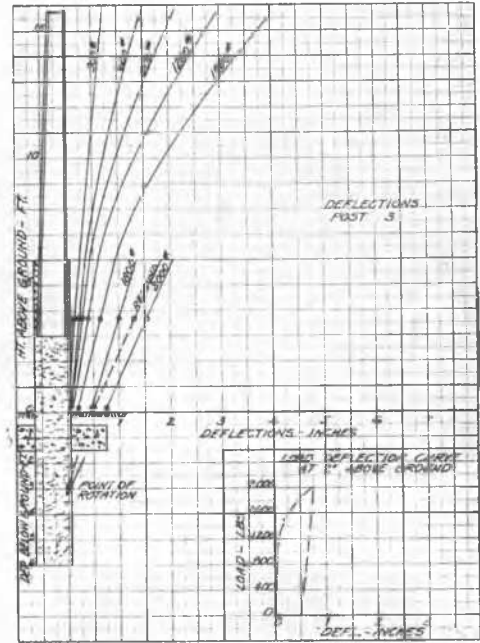


FIG. 4

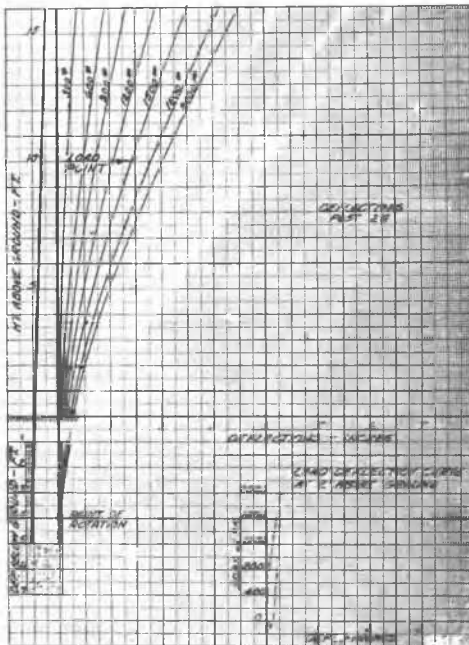


FIG. 3

the ground 18 inches, measuring the pull needed to raise the auger 6 inches, then turning the auger down to 24 inches, measuring the pull needed to raise it 6 inches, and repeating for each six inches of depth up to six feet. The pull was measured with the dynamometer used for post testing and applied with a small chain hoist supported on a tripod. The results of the pilot auger tests are not included in this report because of lack of space.

LABORATORY TESTING

For the laboratory tests, posts one-fourth the size of those used in the field tests and of varying cross-sections were embedded in a fine sand to depths of 15, 18, 24, and 30 inches.

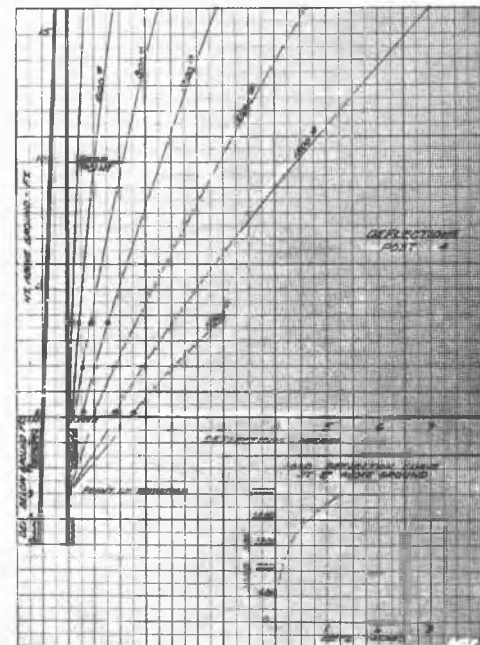


FIG. 5

es. The sand was compacted to a density of approximately 107 pounds per cubic ft. in a wooden box 18 inches wide and 36 inches long and 36 inches deep. Load was applied to the post in 5 pound increments at a height of 30 inches above the sand by means of a cable, pulley, and weights. Deflections of the embedded portion of the posts were measured by means of long thin rods in hollow tubes embedded in the sand and extending out to standard dial gauges. Plate 3 is a photograph of the laboratory equipment.

FIELD TEST RESULTS

The field test results are presented in plotted form on Figures 1 to 13. Each figure

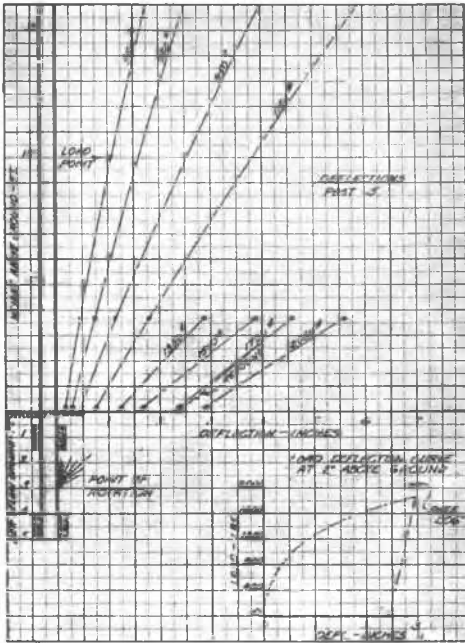


FIG. 6

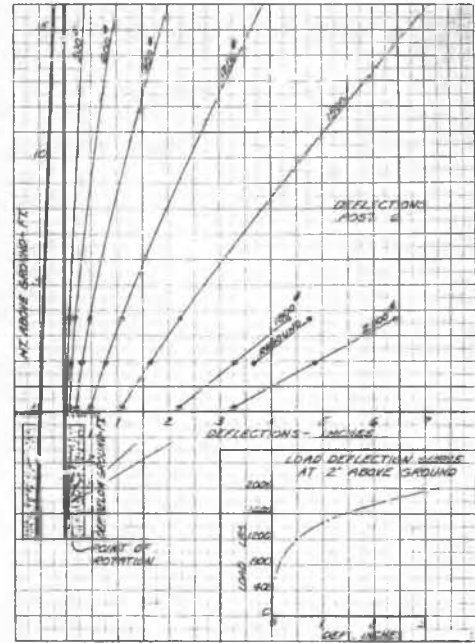


FIG. 8

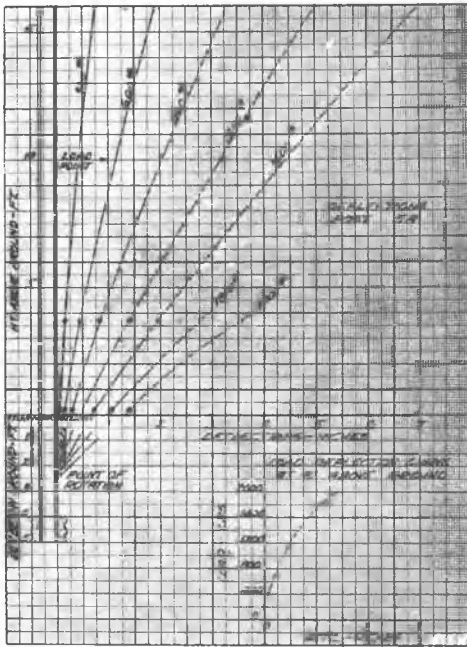


FIG. 7

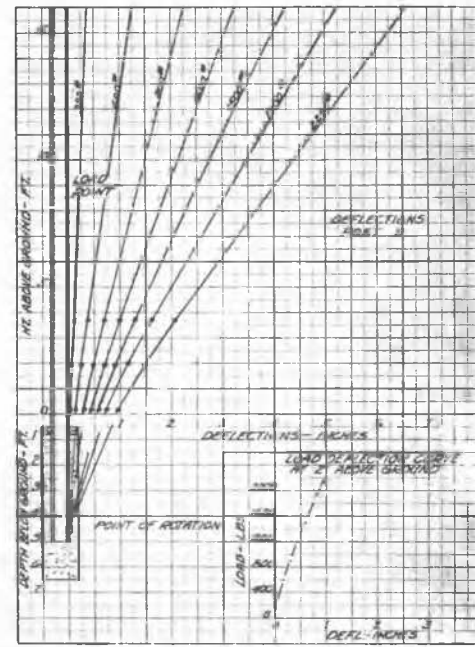


FIG. 9

shows two plots: one of load versus deflection for the gauge nearest the ground surface and one of the deflections of all gauges and the post top for the first loading increments up to 2000 pounds. The last named curves were corrected to straight lines by subtracting the bending in the post and these straight lines were projected to a common intersection with the original position of the post thus locating the point of rotation. Deflections for opposite direction and repeated loadings are not given in this report because of space limitations.

The depth of embedment, water content of the soil, and the type of each post are shown in Table 1. The Omsted Post is a fabricated

galvanized sheet metal I-Beam of the form and dimensions shown on Figure 18. All posts set in pipes had the space between pipe and post filled with dry sand and capped with a concrete cap 3 inches thick. The wings of Posts 4, 5, 5A, and 13 were 3 inch thick planks bolted to both flanges of the post in such a manner that the top of the wing was 6 inches below the ground surface and the larger dimension was horizontal. In addition to the wings, the bottoms of Posts 4, 5, and 5A were set in a 12 inch length of 15 inch diameter corrugated pipe with the space between pipe and post filled with dry sand. Post 13 had wood wings 1 ft. x 1 ft. x 3 in. thick placed against but not bolted to the flanges at the bottom of the

TABLE 1

DEPTH OF EMBEDMENT, WATER CONTENT OF SOIL AND POST TYPE FOR FIELD POSTS			
Post No.	Depth of Embedment Feet	Average Water Content of Soil, Per Cent 0-4 Ft. Depth	Post Type
Test SITE NO. 1			
1	5.00	13.5	Olmsted Post
2	5.75	11.1	Olmsted Post set 5.25 ft. in a 6 ft. length of 14 in. dia 10 gauge steel pipe.
2A	7.00	12.5	Olmsted Post set 4 ft. in a 6 ft. length of 14 in. dia. 10 gauge steel pipe.
3	6.00	13.1	Olmsted Post set 3 ft. in a 12 ft. length of 14 in. dia. 10 gauge steel pipe. Concrete collar 1 ft. thick by 3.5 ft. dia. 0.5 ft. underground-
4	5.00	13.1	Olmsted Post with wings 2 ft. x 1.5 ft.
5	5.00	12.4	7 in. steel I-Beam with wings 1.5 ft. x 1.0 ft.
5A	5.00	13.2	7 in. steel I-Beam with wings 2 ft. x 1.5 ft.
6	5.00	13.2	Olmsted Post set in soil-cement 2 ft. dia.
TEST SITE NO. 2			
9	6.5	22.8	7 in. steel I-Beam set 4.5 ft. in a 6 ft. length of 14 in. dia. 10 gauge steel pipe.
10	5.0	22.6	Olmsted Post set in soil-cement 2 ft. dia.
12	8.0	20.6	8 in. steel I-Beam set 3 ft. in a 12 ft. length of 14 in. dia. 10 gauge steel pipe.
13	5.0	21.3	Olmsted Post with wings 2 ft. x 2 ft.
14	6.0	21.2	10 in. steel I-Beam set 5 ft. in a cast-in place concrete pipe 2 ft. dia.

post.

The deflections of Post 6 were affected by the fact that the soil-cement was not mixed properly but was placed in alternate layers of soil and cement. The deflections of Post 2, 3, and 14 were affected by the failure of the concrete cap over the sand filling in the pipe because of insufficient curing. During the process of testing Post 12, it was noticed that free water filled the hole up to 30 inches below the surface.

LABORATORY TEST RESULTS

The laboratory test results are presented in plotted form on Figures 24 to 36. Each figure shows two plots: one of load versus deflection of the dial gauge nearest the surface and one of the deflections of all gauges for representative loads. The common intersection of the latter deflection curves serves to indicate the point of rotation for the embedded portion of the post. The depth of embedment, type of post, and estimated sand density for

each post is given in Table 2. The sand density was estimated from an excess and deficiency record for each filling of the box and from a trial compaction in a standard 0.10 cu.ft. container using the same compaction method employed in filling the box. The I-Beam type of post was designed to be a one-fourth size model of the Olmsted post used in the field tests except that the cross-section was uniform whereas the field post tapered from bottom to top. The thickness of the galvanized steel metal was such that the relative rigidity of the field and laboratory post was approximately the same. The wood wings were of one-quarter inch thick plywood fastened to both flanges of the I-Beam so that the bottom of the lower wing was flush with the bottom of the post and the top of the top wing was one and one-half inches below the sand surface. The dimensions of the wings perpendicular to the direction of motion was 3" x 3" for the bottom wing and 6" x 6" for the top wing. These wings were a one-fourth size reproduction of those on field Post 13.

TABLE 2

DEPTH OF EMBEDMENT, TYPE OF POST AND SAND DENSITY FOR LABORATORY POSTS			
Post No.	Depth of Embedment Inches	Type of Post	Estimated Sand Density Pounds per cu. ft.
17	18	3" Fabricated I-Beam	106
18	24	3" Fabricated I-Beam	106
19	30	3" Fabricated I-Beam	107
20	30	3" Fabricated I-Beam	107
21	30	3" Fabricated I-Beam	102
22	24	3" Fabricated I-Beam	107
23	24	3" Steel Boiler Tube 1/8" Walls	106
24	24	3" Fabricated I-Beam With Wood Wings	106
25	24	3" Square Wood	106
26	18	3" Fabricated I-Beam With Wood Wings	108
27	15	3" Fabricated I-Beam With Wood Wings	108
28	15	3" Square Wood	108
29	18	1/2 of 3" Dia. Round Wood	108

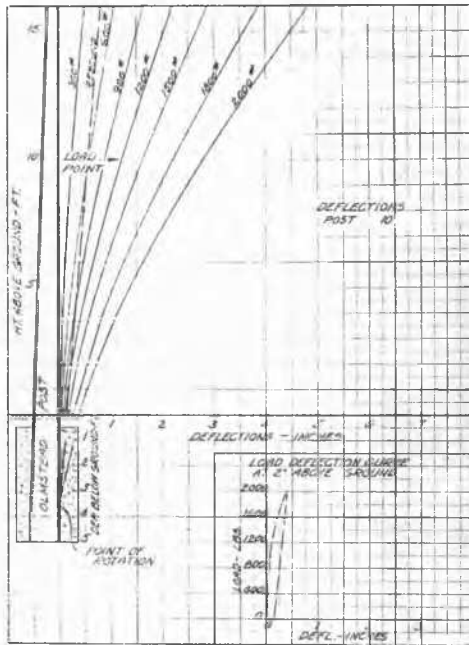


FIG. 10

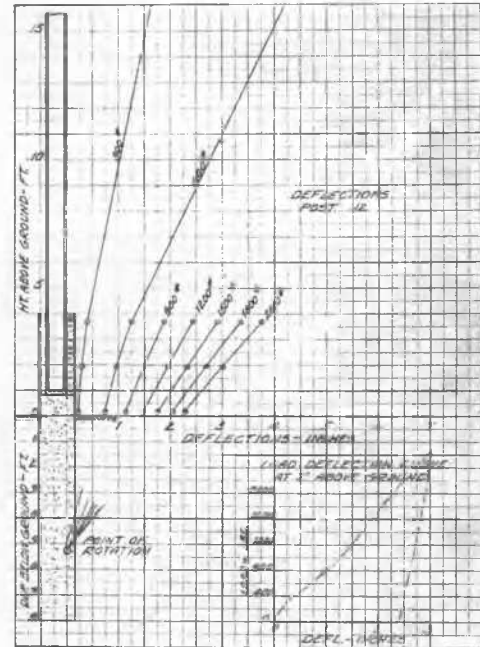


FIG. 11

DISCUSSION OF FIELD RESULTS

The results of the field tests as presented show the deflection of the various posts in the soils of the test sites, but the prediction of the deflection of other posts in the same or other soils requires an analysis of the results and an evaluation of the effect of post dimensions, depth of embedment, and soil type on those results. The theory of such an analysis is that the pull of a lateral load on a post causes the post to rotate in a vertical plane about some point along the embedded portion of the post and that this movement develops a resistance of the soil in opposite directions above and below the point of rotation. The movement of the post will stop when the moment caused by the load is balanced by the moment of the resistance forces in the soil. In order to use this theory, the location of the point of rotation and the amount and distribution of the soil resistance must be known. A location for the point of rotation is given by Seiler in the article mentioned in the introduction. His paper contains a drawing showing the location of the point of rotation to be 0.676 of

the depth of embedment below the ground surface and indicating that the soil resistances are so distributed that they may be represented by a resultant force at 0.338 of the depth of embedment below the surface and a resultant force at 0.898 of the depth of embedment below the surface. A comparison of Seiler's location with the measured location of the points of rotation on Figures 1-13 indicated considerable variation. This fact together with the irregular shape of the embedded portion of the test posts led to the idea that the location of the point of rotation should be based on the area of a vertical cross-section (perpendicular to load direction) of the embedded portion of the post and a computation was made to find that depth above which there was 0.676 of this cross-sectional area. This depth checked very well with the measured locations for Test Site 2 where the soil was uniform, but did not compare so favorably with those for Test Site 1 where a decided change in soil occurred at a depth of four feet. Visual analysis, soil gradation and density, and pilot auger tests at Test Site 1 indicated that the soil below a depth of four feet would have much less resistance than the

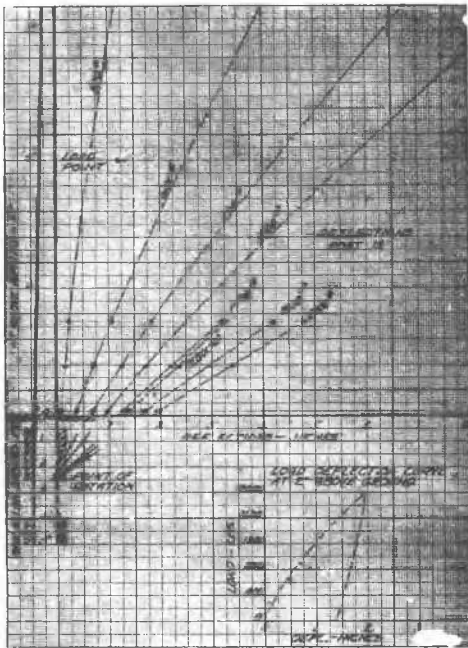


FIG. 12

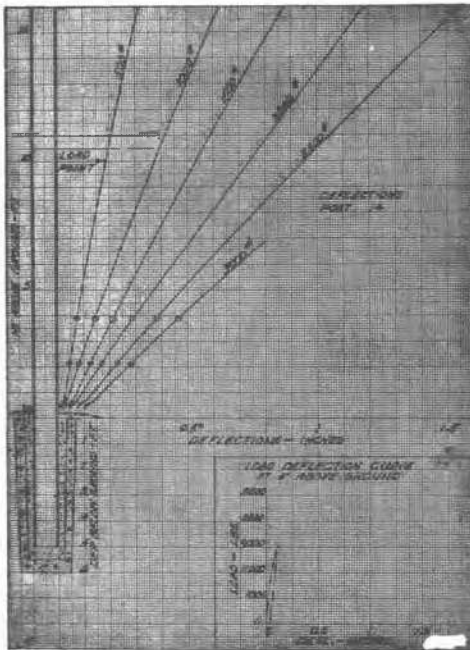


FIG. 13

upper soil; and it was estimated to be one-half as much. Therefore, another calculation was made to locate the point of rotation after adjusting the cross-sectional area by reducing the width of the post cross-section below four feet to one-half its true value and placing the point of rotation at a point above which there was 0.676 of the adjusted area. The results of this calculation checked rather well with the measured locations except for the Olmsted and I-Beam posts where a further adjustment of area appeared necessary. By trial, it was found that, if the cross-section of this type of post was assumed to be equal to that of a round post of the same diameter as the depth of beam, the calculated locations for the point of rotation

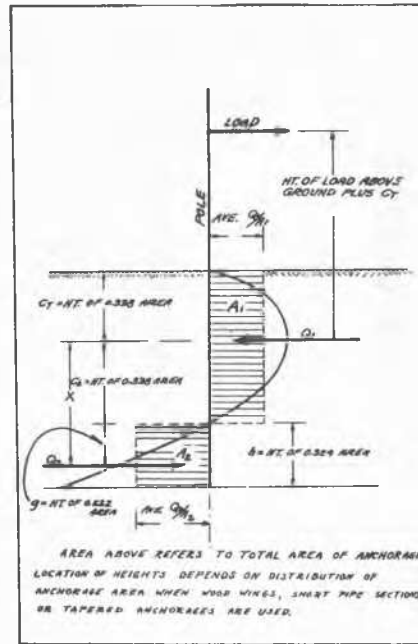


FIG. 14

checked the measured locations. This assumption was later justified by the laboratory tests (Compare Posts 22 and 23 Figures 29 and 30). The calculated and measured locations now all checked except those for Post 6 where the progressive disintegration of the soil-cement made any assumption of its cross-sectional area very difficult. The comparison between computed and measured locations of the point of rotation are shown below :

Post No.	Measured Depth, Ft.	Calculated Depth ft.
1	3.10	3.04
2	---	3.28
2A	3.90	3.90
3	2.90	2.83
4	2.90-2.55	2.64
5	2.90-2.70	2.91
5A	2.30	2.25
6	3.70-3.50	----
9	4.50	4.48
10	3.50	3.50
12	5.30-5.10	5.41
13	2.40-2.20	2.73
14	---	4.15

Such encouraging results for the location of the point of rotation led to a hope of evaluating the effect of soil resistance. A concept of the soil resistance was borrowed from a preliminary analysis of the test data from Site 1 made by Dr. P.C. Rutledge. In the analysis, he compared post deflection to an average soil pressure computed by assuming the point of rotation to be at a depth of 0.7 of the embedment and the resistance forces to act at depths of 0.4 and 0.9 respectively and then computing an average unit pressure by dividing the upper resistance force by the cross-sectional area between a depth of 0.1 and 0.7 of the embedment. This average pressure was not intended to represent a true soil stress but did offer a means of comparing post action. It

TABLE 3
AVERAGE SOIL PRESSURE COMPUTATIONS

Post No.	Anchorage Area	h	g	c _b	x	c _t	Moment	d ₂	d ₁	Bottom area	Top area	Average Soil Stress		Defl. at grnd.
												Bot.	Top	
1	4.50	1.96	1.04	1.52	2.56	1.52	24192 x)	9450	11550	1.46	3.04	6470	3800	3.351
2	5.69	2.47	1.44	1.65	3.09	1.63	23260	7520	9520	1.84	3.85	4080	2470	1.030
2A	5.75	3.10	2.08	1.66	3.74	2.24	24480	6550	8550	1.86	3.89	3520	2190	.271
3	7.84	3.17	1.82	1.64	3.46	1.19	38380	11100	13100	2.54	5.30	4370	2470	.749
4	6.12	2.36	1.36	1.35	2.71	1.29	22580	8330	10330	1.98	4.14	4200	2500	1.269
5	3.86	2.09	1.46	1.73	3.19	1.18	22360	7000	9000	1.25	2.61	5600	3450	2.880
5A	5.07	2.75	1.91	1.03	2.94	1.22	22440	7650	9650	1.64	3.43	4660	2810	1.405
6	6.00	1.42	0.81	1.01	1.82	2.57	23140	12700	14700	1.95	4.05	6500	3640	3.265
9	7.29	2.02	1.39	2.11	3.50	2.37	25014 xa)	7150	9350	2.36	4.93	3030	1895	0.946
10	9.50	1.54	1.05	1.60	2.65	1.86	23720	8950	10950	3.08	6.42	2900	1708	.390
12	9.33	2.59	1.77	2.70	4.47	2.71	53420	11920	13920	3.03	6.30	3940	2210	2.267
13	7.00	2.27	1.55	1.30	2.85	1.43	22860	8030	10030	2.27	4.73	3530	2120	1.965
14	10.35	1.85	1.26	1.86	3.12	1.79	24580	7880	9880	3.36	6.99	2350	1415	.043

x) 2100 pound load
xa) 2200 pound load

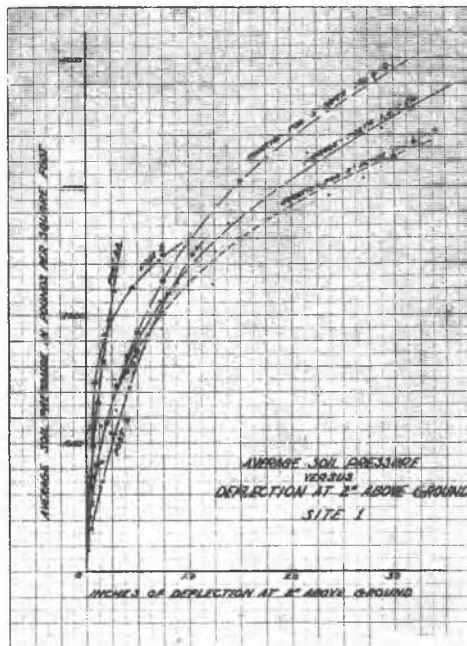


FIG. 15

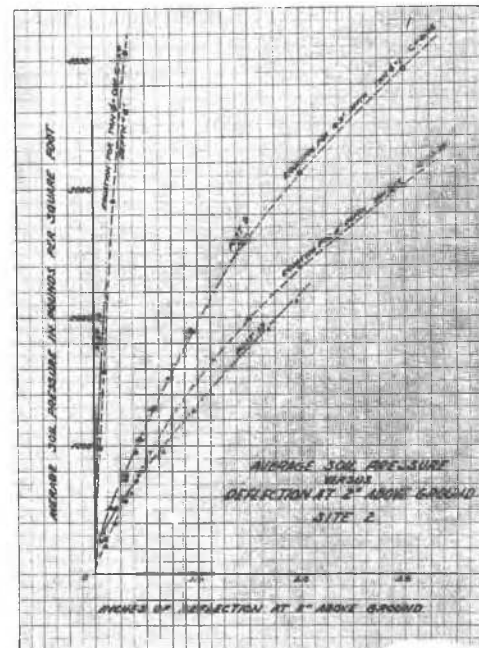


FIG. 16

seemed logical to modify Dr. Rutledge's assumptions by making the point of rotation conform to our calculated and checked location of the point of rotation and by using Seiler's location of forces as modified since that location of the point of rotation appeared correct. This was done and a computation was made to find the average soil pressure using the assumptions shown in Figure 14 with the results shown in Table 3. A plot was made of the average pressure Q_1/A_1 versus the movement of the post at two inches above ground with results as shown in Figure 15 and 16. For the original report,

the Outdoor Advertising Association was interested in the movement of posts subjected to a 2000 pound load and it was found from Figures 15 and 16 that the relation of average soil pressure to post movement for a 2000 pound load could, for practical purposes, be represented by a straight line for each soil. However, it appeared to the authors that a laboratory investigation, being under more controlled conditions, might allow a more fundamental relation to be developed to include any load and any soil. It was with this thought in mind that the laboratory results were studied and the following analysis made.

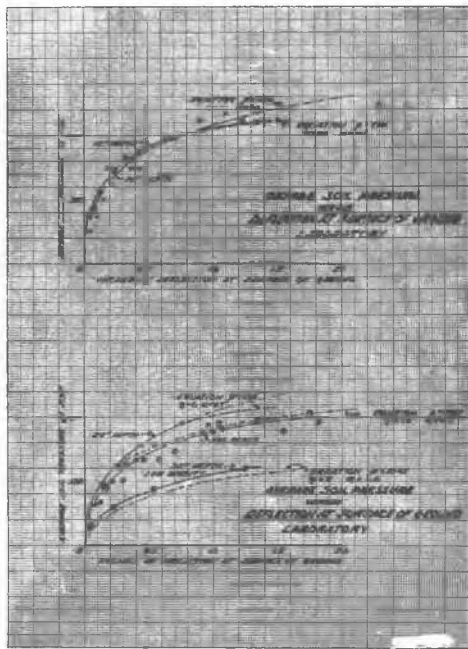


FIG. 17

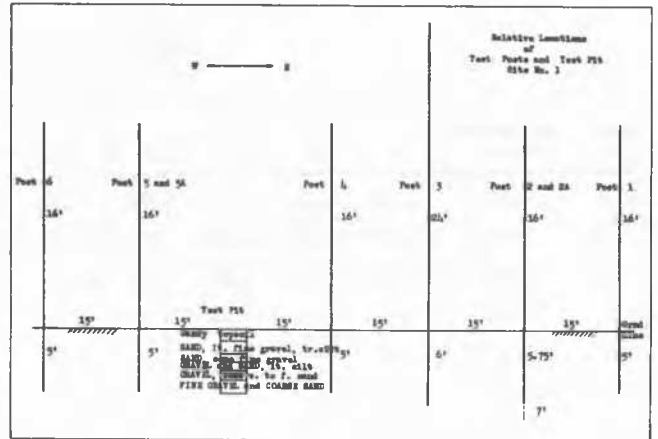


FIG. 19

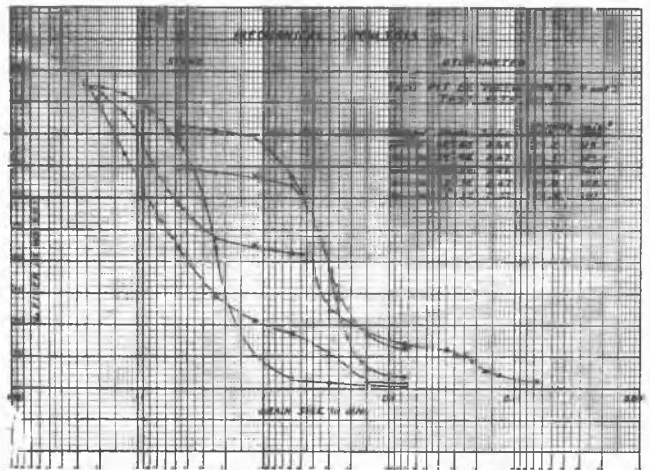


FIG. 20

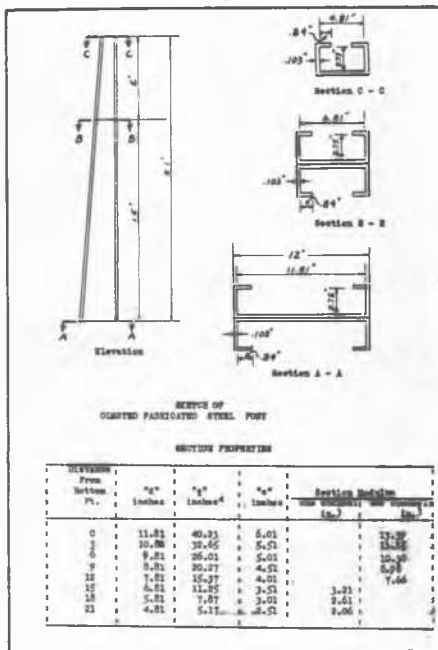


FIG. 18

DISCUSSION OF LABORATORY RESULTS

Results of the laboratory tests allow an interesting comparison of the movement under load for posts of various shapes and also provide justification for the assumptions made in the analysis of the field results. Posts 22 and 23, a 3 inch round section and a 3 inch I-Beam section, respectively, had very similar resistance to loads thus justifying the assumption made in the analysis of field results. Figures 30 and 32, show that a 3 inch square section moves less under load than a 3 inch round section and a computation of their average pressures indicated that the 3 inch square section acts approximately as a round section of

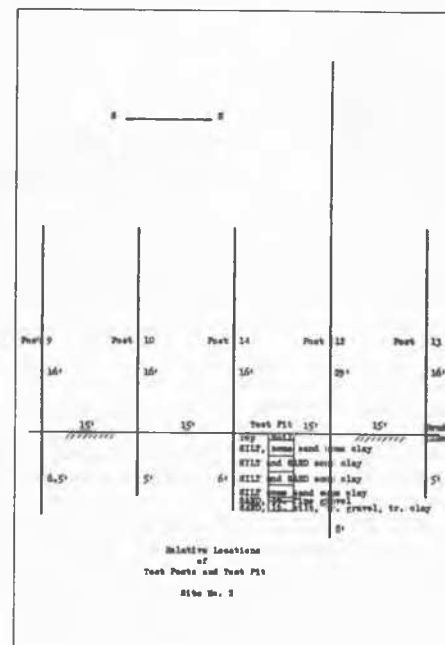


FIG. 21

TABLE 4

SUMMARY SHEET - TRIAXIAL COMPRESSION TESTS ON COHESIVE SOILS

Laboratory or Job Number N - 16

Name of Soil SOUTH BEND SILTY CLAY

Purpose of Tests STRENGTH CHARACTERISTICS

Special Conditions OAA POLE STABILITY TEST SITE NO. 2

1	2	3	4	5	6	7	8	9	10	11	12	13	14	15	16	17	18	19	20	21	22	23	24	25	26	27																							
																											INITIAL CONDITION OF SPECIMEN						TIME ALLOWED FOR				CONSOLIDATION		CONDITIONS AT END OF TEST				COMPRESSION STRESSES KG. PER SQ. CM.				FAILURE		DESCRIPTION OF TESTING EQUIPMENT
																											APPLICATION OF AXIAL LOAD																						
																											ROUTINE TEST RESULTS																						
ROUTINE TEST RESULTS	Diameter of Specimen	Height of Specimen	Initial Water Content	Initial Void Ratio	Initial Dry Unit Weight	Initial Degree of Saturation	Prelim. Consolidation Aver. per Increment	Total for Preliminary Consolidation	To Max. (σ_{1-3})	From 90% to 100% of Max. (σ_{1-3})	Total for Compression	Number of Consolidation Increments	Maximum Consolidation Pressure	Void Ratio After Prelim Consolidation	Strain at Max. (σ_{1-3})	Strain at End of Test	Water Content at End	Void Ratio at End of Test	Degree of Sat. at End	Minor Principal Stress	Strength-Max. (σ_{1-3})	Max. Major Principal Stress	Modulus of Deformation	Measured Slope of Shear Plans	Sketch Showing Type of Failure																								
SAMPLE TEST NUMBER	D _o	H _o	W _o	e _o	γ _d	S _o	Minutes					kg/cm ²	e _c	%	%	%	e	%	σ ₃	Δσ	σ ₁	E	α _o		REMARKS SPECIAL CONDITIONS OF TESTS																								
S-1	REDDISH BROWN SILTY CLAY WITH FINE SEAMS OF GREY SILT & LENSES OF SILTY SAND - HETEROGENEOUS, IRON OXIDE CONCRETIONS, MANY CRACKS																								s = 2.66																								
Q11	3.64	7.87	18.4	.608	104.2	81.4									1.5	1.8	18.0			0	1.80	1.80																											
	3.56	7.23	19.0	.726	97.2	70.3									3.9	6.7	18.7			0.5	2.00	2.50																											
	3.57	7.61	18.1	.662	100.8	73.4									9.5	9.5	17.6	.573	81.0	2.0	4.14	6.14																											
	3.49	7.02	17.4	.556	108.8	83.1									9.1	10.0	16.8	.545	83.0	1.0	4.28	5.28																											
S-2	SIMILAR TO S1 - ROOT HOLES INTO WHICH PARAFFIN PENETRATED - SMALL STONES TO 1/4" DIAM.																								s = 2.65																								
U2	3.55	7.03	17.2	.577	105.0	78.7									1.1	2.0	16.8			0	1.14	1.14																											
Q6	3.58	7.74	17.2	.530	108.1	86.0									2.0	3.0	17.0			0.5	2.59	3.09																											
	3.53	7.03	16.2	.528	108.5	81.2									4.7	10.0	15.7	.515		2.0	4.44	6.44																											
S-3	LIGHT BROWN CLAYEY SILT WITH NUMEROUS NATURAL CRACKS & OCCASIONAL STONES TO 1/4" DIAM.																								s = 2.71																								
U3	3.58	6.95	22.0	.673	101.2	89.0									1.9	2.7	21.6	.672	87.2	0	0.50	0.50																											
Q5	3.52	6.96	21.2	.652	102.4	88.7									2.0	2.9	20.9	.645	87.9	0.5	0.70	1.20																											
Q6	3.48	6.87	20.5	.610	105.4	91.7									1.8	3.1	19.9	.564	95.7	2.0	0.91	2.91																											
Q12	3.56	6.40	22.3	.641	103.0	94.3									2.4	4.0	21.9	.608	97.5	1.0	0.59	1.59																											
S-4	FIRM CRUMBLY BROWN CLAYEY SILT WITH NATURAL CRACKS AND STONES TO 1/4" DIAM.																								s = 2.73																								
U4	3.52	7.00	13.4	.435	118.9	83.8									1.3	2.2	13.2			0	2.68	2.68																											
Q7	3.56	7.00	13.2	.404	121.5	89.8									1.8	2.6	12.9	.404	86.8	0.5	4.20	4.70																											
Q8	3.56	7.00	13.5	.416	120.5	89.0									2.2	8.9	13.3			2.0	5.15	7.15																											
	REMOVED - MIXTURE OF S-2 AND S-3 AT NATURAL WATER CONTENT WITH MODERATE COMPACTION INTO SPECIMEN MOLD																								s = 2.68																								
U5	3.65	6.60	19.5	.557	102.6	93.5									13.4	13.8	18.9	.557	91.2	0	0.50	0.50																											
Q9	3.56	6.92	19.2	.544	108.4	94.6									8.1	8.1	18.7	.544	92.1	0.5	0.50	1.00																											
Q10	3.59	6.82	19.4	.561	107.1	92.3									9.9	10.1	18.7	.512	98.5	2.0	0.61	2.61																											

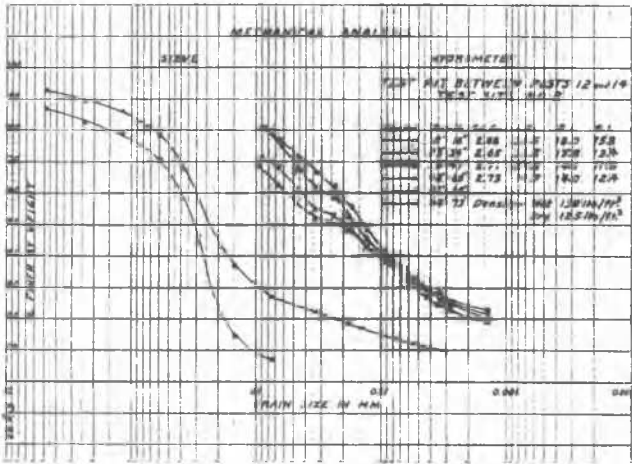


FIG.22

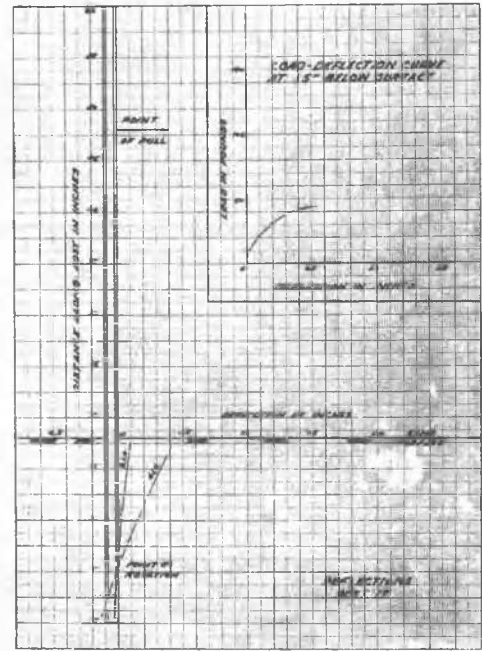


FIG.24

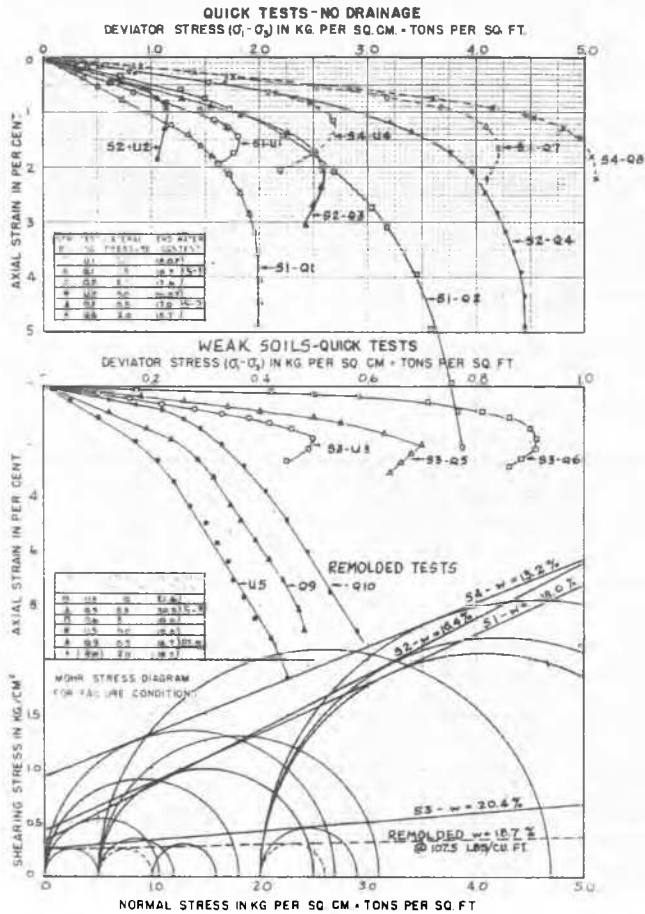


FIG. 23

TRIAxIAL COMPRESSION TEST STRESS-STRAIN CURVES

SAMPLE NOS. 1 THRU 4 PROJECT N-16
LOCATION OAA POLE STABILITY TEST SITE NO.2-SOUTH BEND, INDIANA

504 MECHANICS LABORATORY TECHNOLOGICAL INSTITUTE NORTHWESTERN UNIVERSITY

FIG.23

a diameter equal to the diagonal of the square. The half round section of Figure 36 shows slightly greater resistance to load than a full round section. Comparison of Figures 24, 29, 31 and 33 shows that the wings on Posts 24 and 26 affect the position of the point of rotation and the resistance to load in the same manner

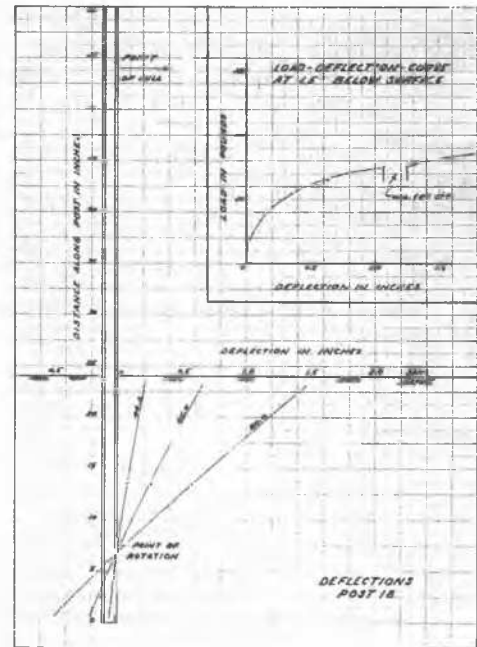


FIG. 25

as was assumed in the analysis of field results.

The laboratory results also indicate some trends concerning the point of rotation. The position of the point of rotation drops with increasing depth of embedment. However, this tendency may have been influenced by the restraining effect of the box since the position for shallower depths does correspond with locations as found in the field tests. There was also some indication that the point of rotation might be lowered by decreasing densities.

The above observations were interesting but were of secondary consideration to establishing the general relation between pressure and movement. To do this, a calculation was made of the average pressure using the measured

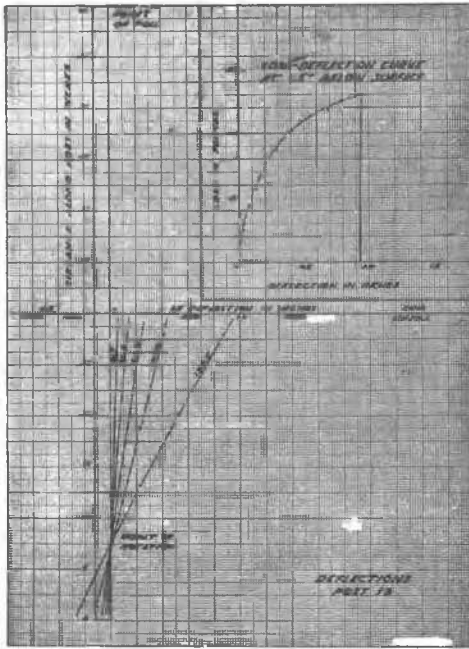


FIG. 26

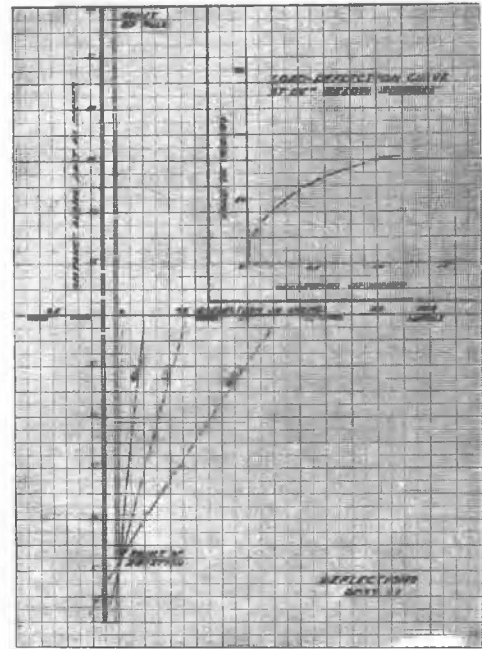


FIG. 28

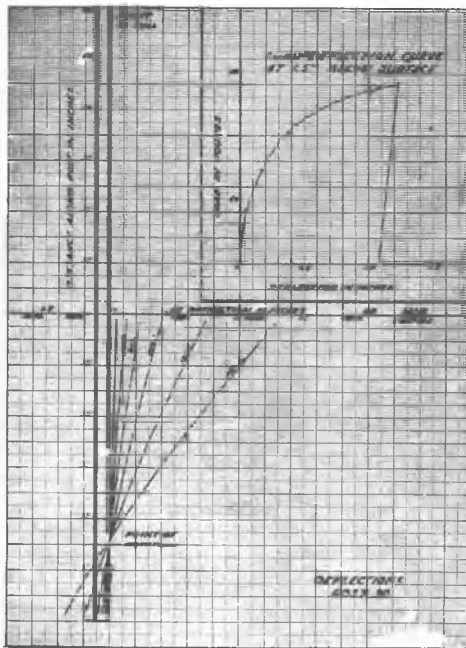


FIG. 27

location of the point of rotation and the assumptions of Figure 14 and a plot was made for each post of average pressure versus movement of the post at the sand surface. It was noticed that when the curves were plotted on log paper, a straight line resulted for small deflections, and when they were plotted on semi-log paper, a straight line resulted for the larger deflections. This suggested that the early part of each curve was a power function and the latter part an exponential function. Dr. Paul Pepper, Professor of Mathematics at the University of Notre Dame, suggested that an equation of the form $y = \rho \log(1 + \beta x^{\alpha})$ would describe such curves. In this equation, y represents the average pressure and x the

deflection. The constant ρ is a scale factor controlling the vertical position of the curve; the constant α controls the general slope of the curve; and the constant β controls the change in curvature.

A trial procedure established the fact that the following values of ρ , β and α would cause the equation to describe the average experimental curve for each of the depths of embedment (See Figure 17):

For 15" depth;	$\rho = 735$,	$\beta = 25$,	$\alpha = 0.7$
For 18" depth;	$\rho = 1040$.	$\beta = 10$,	$\alpha = 0.7$
For 24" depth;	$\rho = 789$,	$\beta = 13$,	$\alpha = 0.7$
For 30" depth;	$\rho = 1230$,	$\beta = 6$,	$\alpha = 0.7$
For 30" depth (low density)	$\rho = 1045$,	$\beta = 2$,	$\alpha = 0.6$

The value for α apparently varied with the sand density and seemed to be equal to a reasonable value for the tangent of ϕ (the angle of internal friction) for the sand used in the experiment. The value of β seemed to get smaller as the depth of embedment increased; but the variation was not constant because it was necessary to vary ρ in a somewhat inconsistent fashion for the 15 and 18 inch depths. However, for the 24 and 30 inch depths, the value of ρ was equal to P_p (Rankine's pas-

sive pressure for the depth in question) and the values of β seemed to vary with the depth and density.

A second trial procedure of fitting the equation to the experimental curves for Test Site 1, disclosed that the equation would describe within reasonable limits the average experimental curve for each depth of embedment if ρ was made equal to P_p , β was made equal to two and α was made equal to a reasonable value of the $\tan \phi$ for the granular soil. The curves of Figure 15 show the comparison between the average experimental curve for a 5 ft. depth of embedment and curves of the equation for the same embedment using values of 0.6 and 0.7 for α .

A third trial procedure of fitting the

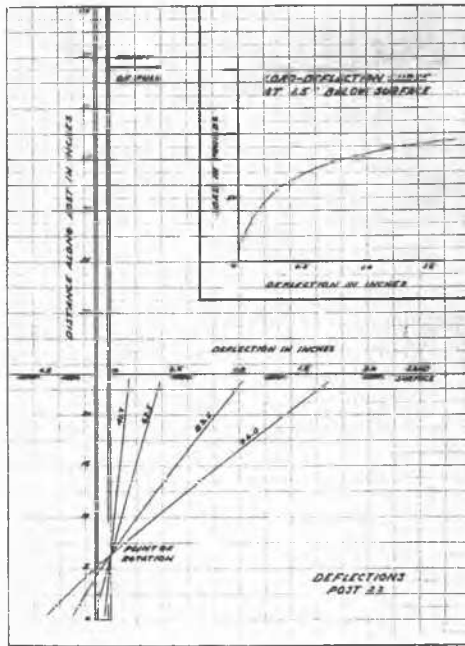


FIG. 29

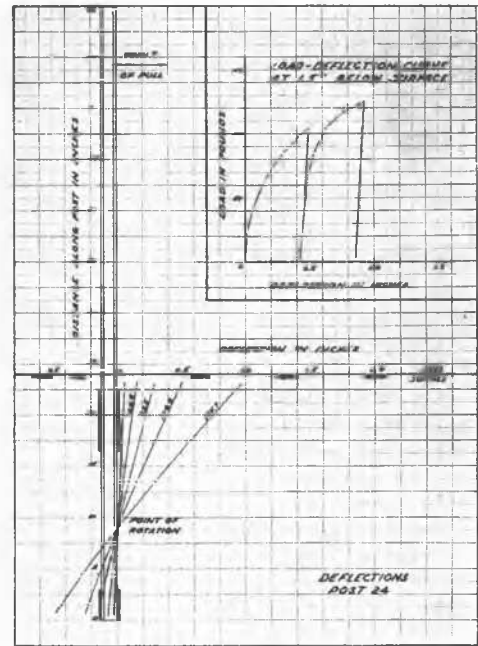


FIG. 31

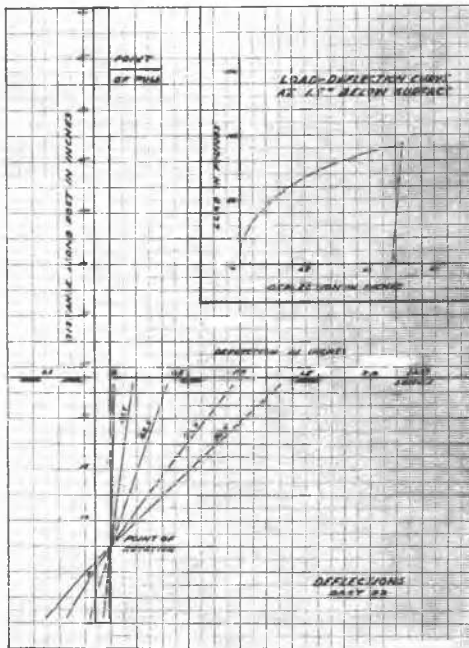


FIG. 30

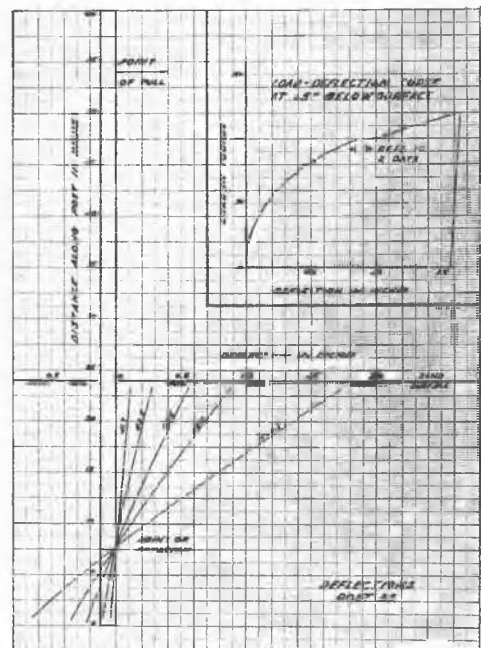


FIG. 32

equation to the experimental curves for Test Site 2, developed the fact that the equation would describe the curve for Post 14 if the $\tan \phi$, Figure 23, for the soil was replaced with a $\tan \phi'$ which would give a "passive pressure" value at the bottom of the post equal to that computed using both ϕ and the cohesion. The cast-in-place concrete pipe for this post caused the load to be resisted by undisturbed cohesive soil. However, the design of Post 9, 12, and 13 was such that tamped refill soil was adjacent to the post and thus the load was resisted by remolded cohesive soil. For this condition, the exponent of the deflection did not seem related to $\tan \phi$, which according to Figure 23 would be zero, but appeared to cause

the equation to best describe the experimental curve when given a value of one if at the same time the coefficient of the deflection were one. See Figure 16 for a comparison of the curves. The free water in the hole of Post 12 appeared to cause its deflections to be considerably greater than the values given by the equation. The deflections of Post 10, whose backfill was tamped soil-cement appeared to follow a pattern somewhere between a post depending on undisturbed soil and one depending on remolded soil. This appears possible when it is remembered that the soil-cement mixture used for backfill was mixed manually and, consequently, was not of uniform composition.

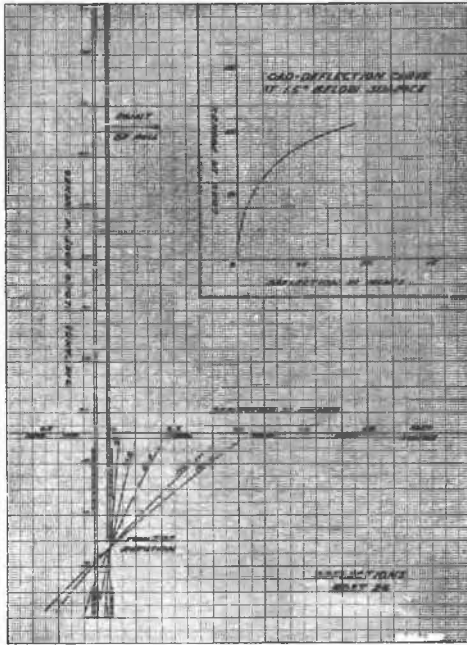


FIG. 33

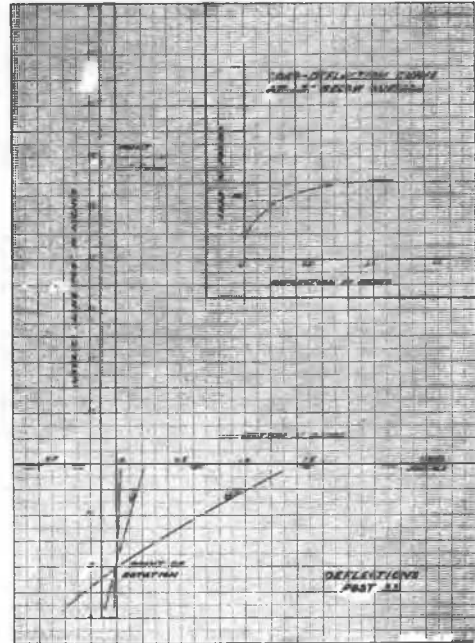


FIG. 35

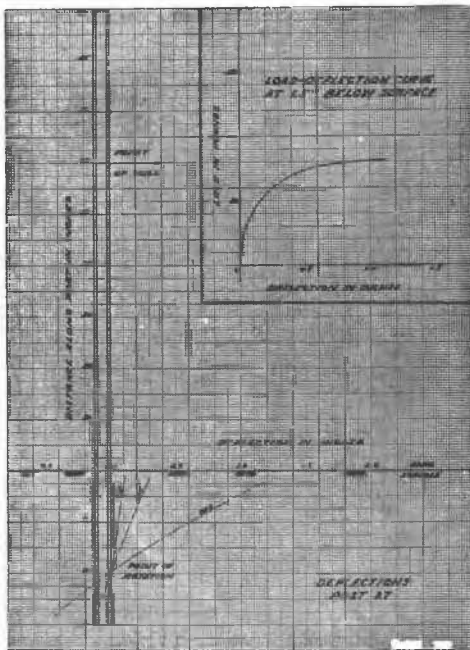


FIG. 34

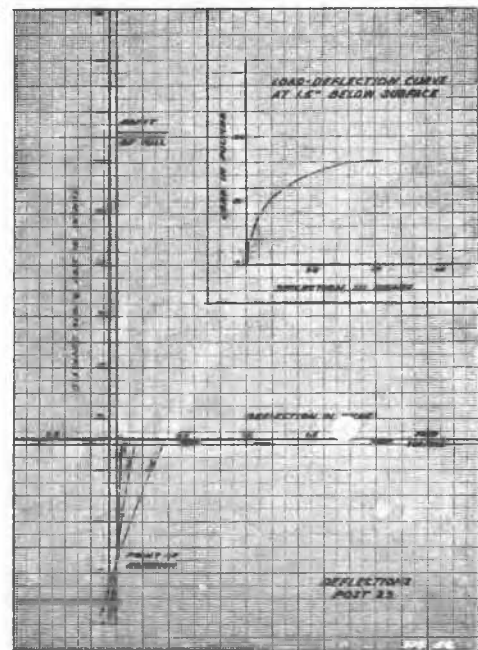


FIG. 36

CONCLUSIONS

The following conclusions are derived from the test results and the discussion thereof. Their validity is limited by the scope of the investigation and the relatively small number of individual posts tested.

- 1) For normal post depths, the location of the point of rotation is at that depth below which there is 0.324 of the total vertical cross-sectional area of the embedded portion.
- 2) The above mentioned location may be lowered by increased depths or very low densities.
- 3) The shape of the embedded portion of the post has a marked effect on its resistance to movement; i.e., I-Beam sections have as

much resistance as round sections of a diameter equal to their depth and square sections have as much resistance as round sections of a diameter equal to the diagonal of the square.

- 4) The resistances of posts to movement under lateral loads can be compared on the basis of an average soil pressure computed as shown in Figure 14.
- 5) For granular soils, and ordinary post depths, the relation between the movement of the post at the ground level and the average soil pressure caused by a lateral load is described by the following equation:

$$\frac{Q_1}{A_1} = P_p \log (1 + 2 \Delta \tan \phi)$$

where $\frac{q_1}{A}$ is the average soil pressure (fig. 14)
 p_p is Rankine's passive pressure
 Δ is the movement of the post at ground level
 φ is the angle of internal friction of the soil.

- 6) The above equation will describe the relation between the movement of the post and the average soil pressure is an undisturbed cohesive soil if φ is replaced by a φ' of such value that the Rankine passive pressure value of the bottom of the post is the same when computed using φ' alone or using the actual φ and the cohesion of the soil.
 7) For posts depending on remolded cohesive soil

for their support, the equation must be further modified by making the exponent of Δ equal to one and changing the coefficient of Δ to one.

- 8) The above equation, with the proper constants, offers a rational means of designing posts and anchorages against relatively small movement under lateral loads.

ACKNOWLEDGEMENTS

The writers wish to thank the Outdoor Advertising Association of America for initiating the tests and allowing the use of the field test data in this report. The writers also wish to thank Dr. F.C. Rutledge of Northwestern University for his helpful advice as a consultant on the field tests and his friendly encouragement of the preparation of this paper.

-o-o-o-o-o-o-o-

V b 9

ABOUT THE CALCULATION OF ANCHORED BULKHEADS WITH FIXED EARTH SUPPORT

R.N. DAVIDENKOFF

Berlin, Degebo

There are as you know for the practical application in the case of cohesionless soils two methods of calculation, i.e. of the ascertainment of the ramming depth (depth of penetration) and cross-section of bulkhead and of the tension in anchor: the method of Krey and the method of Blum x). The first method has to do with so called bulkheads with free earth support, the second method with bulkheads with fixed earth support. In the general case, without consideration of the friction between bulkhead and soil, Krey supposes that it is possible to represent the passive earth pressure before the bulkhead in a simpler manner by the trapezoid-shaped area EFK (Fig. 1a). This passive earth pressure depends on the movements of the bulkhead. Krey does not try to find out the quantitative proportion of this dependence, but easily proves that qualitatively with increasing t f decreases and with decreasing t f increases until with a certain depth, $t = t_1$, the passive earth pressure before the bulkhead is completely utilized (Fig. 1b). The method of Krey is applicable in such cases where t is not too large compared to t_1 (see below the values of the factor of safety.)

With the ascertainment of the ramming depth of bulkhead Krey recommends to utilize only a certain part of the entire area JRK; the factor of safety is then equal (see Fig. 1a) to

$$n = \frac{\text{area JRK}}{\text{area EFKJ}} = \frac{t^2}{t^2 - t_1^2}$$

The equations for the ascertainment of the ramming depth of bulkhead t and the tension in the anchor A with a factor of safety n are as follows (γ = unit weight of the homogeneous soil, S_a and S_p = coefficients of the active and passive earth pressure):

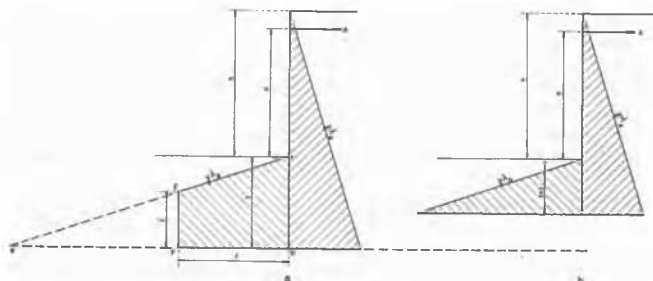
$$\frac{\gamma S_a (h + t)^2}{2} - A - \frac{\gamma S_p t^2}{2n} = 0$$

$$\frac{\gamma S_a (h + t)^3}{6} - A(g + t) - \frac{\gamma S_p t^3}{6} \left[1 - \left(\frac{n+1}{n} \right)^3 \right] = 0$$

Krey does not give numerical values for n . It may be mentioned here that without consideration of the friction between soil and bulkhead the value $n = 2$ may be accepted as highest value. This is in accordance with other calculations of stability in soil mechanics.

Blum thinks that the safety of the bulkhead calculated according to the method of Krey, is

- x) The method of Freund will not be considered here as it has more theoretical interest: in this method, the practical application of which is very complicated, the coefficient of proportionality between pressure and settlement of soil (such as with beams on elastic foundation) is used, which is not a constant of soil at all.



KREY'S SCHEME OF CALCULATION

FIG. 1